Structural Engineering and Mechanics, Vol. 5, No. 5 (1997) 587-598
DOI: http://dx.doi.org/10.12989/sem.1997.5.5.587

Structural dynamics: Convergence properties in the presence of damage and applications to masonry structures

Alfonso Nappi†, Giovanni Facchin‡ and Claudio Marcuzzi‡

Department of Civil Engineering, University of Trieste, Piazzale Europa 1, 34127 Trieste, Italy

Abstract. A numerical model for masonry is proposed by following an internal variable approach originally developed in the field of elastic-plastic analysis. The general features of the theoretical framework are discussed by focussing on finite element models applicable to incremental elastic-plastic problems. An extremum property is derived and its implications in terms of convergence for convenient algorithms are briefly discussed, by including the case of softening materials and damage effects. Next, a numerical model is presented, which is suitable for masonry, can be developed according to the same internal variable formulation and enjoys similar properties. Some numerical results are presented and compared with the response of a masonry shear wall subjected to pseudodynamic tests.

Key words: backward difference; damage mechanics; extremum properties; internal variables; masonry; plasticity; softening; nonlinear structural dynamics.

1. Introduction

In previous papers (Martin and Reddy 1988, Martin and Nappi 1990, Nappi 1991 and 1995, Rajgelj, *et al.* 1993) an *internal variable* approach for elastic-plastic analysis was discussed, by pointing out convergence properties of algorithms based upon the *backward difference* time integration scheme. In this area, both the *finite element* method and the *boundary element* method were considered. Basic convergence properties, which are of interest for incremental elastic-plastic analysis, essentially depend upon the hypothesis of using *elastic perfectly-plastic* or *elastic hardening* materials, i.e., materials whose behaviour is stable in Drucker's sense (Drucker 1964).

Some emphasis, however, was also given (in the case of finite element discrete models) to the possibility of using the same approach and obtaining the same convergence properties also in the presence of *softening* materials (i.e., *unstable* materials) provided that dynamic actions or viscous effects be taken into account. Indeed, inertia forces, damping and viscosity tend to introduce a stabilising effect. In this way, sufficiently small time increments may ensure convergence of convenient algorithms.

The above concepts are briefly discussed and revisited in the present paper. Next, they are applied to an elastic plastic numerical model, that is characterised by a piecewise linear yield

† Professor
‡ Civil Engineer graduated at the University of Trieste

surface, accounts for damage effects and is suitable for masonry structures. More specifically, the model presented in the paper is meant to describe the macroscopic behaviour of masonry in a simple way and to provide satisfactory results also in the presence of cyclic and dynamic loads. Of course, the simulation of masonry response is a highly difficult task and more sophisticated models may be desirable. A large selection of such models is currently available (see, e.g., Gambarotta and Lagomarsino 1997, Lourenço 1996, Maier, *et al.* 1985 and 1991, Page 1978, Pande, *et al.* 1989, Papa 1996, Papa and Nappi 1997). However, as models become more and more complex the estimate of the relevant parameters often becomes a critical task. A reasonable estimate of such parameters may become even impossible in the case of ancient masonry. As a consequence, there seems to be practical interest in the development of models that represent a reasonable compromise among four key requirements: (i) easy implementation, (ii) estimate of the relevant parameters by means of traditional, simple tests, (iii) possible application to dynamic loads and (iv) capability of describing the overall structural response of masonry structures in terms of displacements, average stresses and damage pattern.

In the following sections, the general features are described of the internal variable approach utilised in the paper and a possible extension applicable to masonry structures is discussed. Next, experimental data provided by a pseudodynamic test on a masonry shear wall are compared with the numerical response obtained by using a simplified (elastic, perfectly plastic) version of the model.

2. An internal variable approach

The internal variable approach followed in the paper was originally developed by Martin (1975, 1981) in the field of Plasticity. The relevant formulation does not make explicit use of yield functions, while a central role is played by the dissipated energy. The basic concepts are easily presented by considering a simple mechanical model subject to uniaxial stress states and concerned with an elastic plastic material characterised by linear kinematic hardening. The model is depicted in Fig. 1. It consists of two elastic springs and one slip device. The stress χ acting on the slip can not exceed given thresholds (χ^+ and χ^-), as shown in Fig. 2. When $\chi=\chi^+$ or $\chi=\chi^-$, unlimited inelastic strain rates $\dot{\lambda}$ are possible. A dissipation function $D(\dot{\lambda})=\chi\dot{\lambda}$ can also be introduced (cf. Fig. 3). The slopes of the straight lines are such that $\chi=dD/d\dot{\lambda}$ when $\dot{\lambda}\neq 0$. On the other hand, χ may attain any value between χ^- and χ^+ when $\dot{\lambda}=0$. Therefore, the response of the model shown in Fig. 1 is governed by the equations

$$\sigma=k\ (\varepsilon-\lambda),\quad -\chi=-k\ (\varepsilon-\lambda)+h\lambda\ \text{ with } \chi=dD/d\dot{\lambda} \text{ if } \dot{\lambda}\neq 0,\ \chi\in\partial D(\dot{\lambda}) \text{ if } \dot{\lambda}=0 \qquad \text{(1a,b,c,d)}$$

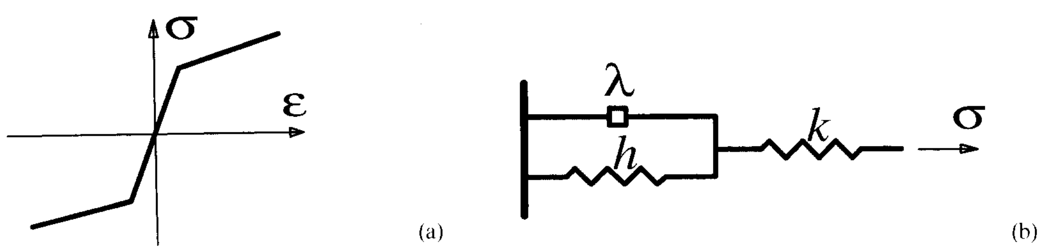

Fig. 1 Stress vs. strain plot for a linear hardening material (a) and mechanical model (b).

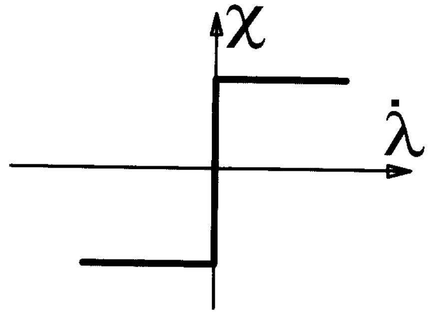

Fig. 2 Stress vs. plastic strain rate plot for a slip device.

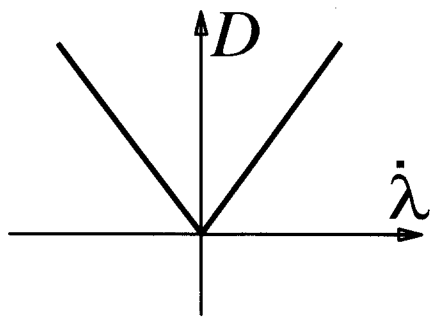

Fig. 3 Dissipation function for a slip device.

where k and h are constant, while the inelastic strain λ represents an *internal*, non measurable variable. In addition, *generalised* stresses σ and strains ε are assumed, so that their product has the physical dimensions of work. Note that similar equations are applicable in the case of *nonlinear* hardening. We only need to introduce a potential function $V(\lambda)$, such that the derivative $(dV/d\lambda)$ denotes the stress acting on the left spring of Fig. 1. Of course, linear hardening simply implies $V(\lambda)=1/2h\lambda^2$.

Similar equations can be obtained in the case of isotropic hardening and of multiaxial stress states, as discussed by Martin and Nappi (1990). The governing equations concerned with multiaxial stresses are substantially identical to Eqs. (1), but convenient matrices ($\underline{k}$, $\underline{h}$) and vectors ($\underline{\sigma}$, $\underline{\varepsilon}$, $\underline{\lambda}$) need to be introduced instead of scalar quantities. Thus, the relevant equations read

$$\underline{\sigma}=\underline{k}\,(\underline{\varepsilon}-\underline{\lambda}),\quad -\underline{\chi}=-\underline{k}\,(\underline{\varepsilon}-\underline{\lambda})+\underline{h}\,\underline{\lambda}\ \text{ with }\ \underline{\chi}=\partial D/\partial\dot{\underline{\lambda}}\ \text{ if }\ \dot{\underline{\lambda}}\neq\underline{0},\quad \underline{\chi}\in\partial D(\dot{\underline{\lambda}})\ \text{ if }\ \dot{\underline{\lambda}}=\underline{0} \quad (2a,\ b,\ c,\ d)$$

Next, it is can be noted that discrete finite element models lead to governing equations which are formally identical at the structural level. Indeed, we may focus on m strain points where the constitutive law is to be enforced. At these points we can assume fictitious slip devices subject to internal forces $\underline{\chi}_j$ conjugate to the internal variables $\underline{\chi}_j$ ($j=1$, ..., m). When $\underline{\chi}_j$ attains convenient values, non-zero rates $\dot{\underline{\lambda}}_j$ are allowed. The relevant dissipation rate will be $D=\underline{\chi}_j^T\dot{\underline{\lambda}}_j$. In addition, $\underline{\chi}_j=\partial D/\partial\dot{\underline{\lambda}}_j$ if $\dot{\underline{\lambda}}_j\neq\underline{0}$. Otherwise, $\underline{\chi}_j$ turns out to represent a subgradient of $D(\dot{\underline{\lambda}}_j)$ when $\dot{\underline{\lambda}}_j=\underline{0}$. Thus, by collecting all the subvectors $\underline{\chi}_j$ into a vector $\underline{\chi}$, the governing equations concerned with the incremental elastic plastic problem read

$$\Delta\underline{F}=\underline{K}\ \Delta\underline{u}+\underline{L}\ \Delta\underline{\lambda},\ -\underline{\chi}=\underline{L}^T\ \Delta\underline{u}+\underline{E}\ \Delta\underline{\lambda}+\{\partial V\partial/\Delta\underline{\lambda}\}+\underline{L}^T\underline{u}_o+\underline{E}\ \underline{\lambda}_o \tag{3a, b}$$

with

$$\underline{\chi}_j=\partial D/\partial\Delta\underline{\lambda}_j\ \text{if}\ \Delta\underline{\lambda}_j\neq\underline{0},\ \underline{\chi}_j\in\partial D(\Delta\underline{\lambda}_j)\ \text{if}\ \Delta\lambda_j=\underline{0} \tag{3c, d}$$

The above equations are written by assuming a load history subdivided into time steps during which finite increments of external actions ($\Delta\underline{F}$), free nodal displacements ($\Delta\underline{u}$) and internal variables ($\Delta\underline{\lambda}$) take place. The vectors $\underline{u}_o$ and $\underline{\lambda}_o$ denote values attained by nodal displacements and internal variables at the beginning of the current interval. In Eq. (3a) $\underline{K}$ is the structural stiffness matrix, while $\underline{L}$ transforms internal variables into equivalent nodal loads. In Eq. (3b) E is a block diagonal matrix that collects the material stiffness matrices $\underline{E}_j$ at the m strain points. Each matrix $\underline{E}_j$ is analogous to the matrix k in Eq. (2b). The gradient $\{\partial V/\partial\Delta\underline{\lambda}\}$ implies the general case of nonlinear hardening. When hardening is linear, that gradient becomes $\{\underline{H}\ \underline{\lambda}_o+\underline{H}\ \Delta\underline{\lambda}\}$, where $\underline{H}=\text{diag}[\underline{H}_j]$ is symmetric and positive definite. Next, by considering Eq. (3c), it is worth noting that, in principle, $\underline{\chi}_j=\partial D/\partial\dot{\underline{\lambda}}_j$. However, by applying the *backward difference* time integration scheme, which implies *straight paths* in the space of the inelastic strain increments, we obtain $\partial D/\partial\Delta\underline{\lambda}_j=\partial D/\partial\dot{\underline{\lambda}}_j$.

Eqs. (3) represent the *optimality conditions* for the *convex, unconstrained problem*

$$\min\left\{\frac{1}{2}\ \Delta\underline{u}^T\ \underline{K}\ \Delta\underline{u}+\Delta\underline{u}^T\ \underline{L}\ \Delta\underline{\lambda}+\frac{1}{2}\ \Delta\underline{\lambda}^T\ \underline{E}\ \Delta\underline{\lambda}\right.$$
$$\left.+D(\Delta\underline{\lambda})+V(\Delta\underline{\lambda})-\Delta\underline{F}^T\ \Delta\underline{u}+\Delta\underline{\lambda}^T\ \underline{L}^T\ \underline{u}_o+\Delta\underline{\lambda}^T\underline{E}\ \underline{\lambda}_o\right\} \tag{4}$$

This extremum property has interesting applications under a computational point of view, since it allows one to obtain a simple, straightforward proof of convergence for classical algorithms based upon a *prediction-correction* technique (Martin and Reddy 1988, Nappi 1991).

Convexity of the function $V(\Delta\underline{\lambda})$ is a basic requirement in order to obtain a convex objective function in the above problem. In the case of *softening* materials and, hence, of non-convex $V(\Delta\underline{\lambda})$ functions, a *regularisation* technique can be adopted, which requires a fictitious viscosity. To this aim, we can consider the model of Fig. 1 and introduce a dashpot in parallel with the left spring and the slip device. Thus, the governing equations becomes

$$\sigma=E(\varepsilon-\lambda),\ -\chi=-E(\varepsilon-\lambda)+h\lambda+z\dot{\lambda},\ \chi=dD/d\dot{\lambda}\ \text{if}\ \dot{\lambda}\neq 0,\ \chi\in\partial D(\dot{\lambda})\ \text{if}\ \dot{\lambda}=0 \tag{5a, b, c, d}$$

where z is a constant parameter that characterises the dashpot response. The above equation can be rewritten in order to include multiaxial stress states. As we did in the case of Eqs. (2), we need to introduce convenient vectors and matrices, including a matrix $\underline{z}$ instead of the scalar quantity z. Next, at the structural level, we derive the equation

$$-\underline{\chi}=\underline{L}^T\ \Delta\underline{u}+\underline{E}\ \ \Delta\underline{\lambda}+\underline{Z}\frac{\Delta\lambda}{\Delta t}+\{\partial V/\partial\Delta\underline{\lambda}\}+\underline{L}^T\underline{u}_o+\underline{E}\ \underline{\lambda}_o \tag{6}$$

that replaces Eq. (3b) and must be used together with Eqs. (3a, c, d). Thus, an optimisation problem can be considered, which is fully analogous to the problem (4), but is characterised by the new term ($1/2\Delta t\ \Delta\underline{\lambda}^T\ \underline{Z}\ \Delta\underline{\lambda}$). Of course, a positive definite matrix $\underline{Z}$ and a sufficiently small time interval Δt may succeed in making the new objective function convex even if $V(\Delta\underline{\lambda})$ is not convex. When the viscous element is utilised with the purpose of developing a regularisation technique, we can proceed as follows. First, for any given increment of the external actions, we solve the problem governed by Eqs. (6) and (3a, c, d). In this way, non-zero plastic strain rates $\{\Delta\underline{\lambda}/\Delta t\}$ are found. Next, we maintain the external actions constant and we continue to solve the same problem until the vector $\{\Delta\underline{\lambda}/\Delta t\}$ is practically zero. Thus, we find the same final conditions which are typical of a traditional elastic plastic analysis performed without considering time-dependent effects. At this stage, the subsequent increment of the external actions can be considered.

In the presence of softening, we may also derive a convex unconstrained problem such as problem (4) by considering dynamic actions. It can be proved that convexity may depend upon the length of the time step Δt, which can often be made small enough to maintain an extremum property and, hence, to ensure convergence. These topics will be briefly summarised in what follows, since the relevent results will be needed in the next section.

In the case of structural dynamics, instead of Eq. (3a) we can write

$$\{\underline{F}_o+\Delta\underline{F}\}=\underline{K}\ \{\underline{u}_o+\Delta\underline{u}\}+\underline{B}\ \{\dot{\underline{u}}_o+\Delta\dot{\underline{u}}\}+\underline{M}\ \{\ddot{\underline{u}}_o+\Delta\ddot{\underline{u}}\}+\underline{L}\ \{\underline{\lambda}_o+\Delta\underline{\lambda}\} \tag{7}$$

where $\underline{B}$ and $\underline{M}$ are the damping matrix and the mass matrix, while $\dot{\underline{u}}$ and $\ddot{\underline{u}}$ denote a velocity vector and an acceleration vector. As usual, $\underline{F}_o$, $\dot{\underline{u}}_o$ and $\ddot{\underline{u}}_o$ represent values at the beginning of the current time step, while $\Delta\dot{\underline{u}}$ and $\Delta\ddot{\underline{u}}$ are convenient increments. Next, by setting

$$\Delta\underline{u}=\dot{\underline{u}}(t^*)\ \Delta t, \qquad \Delta\dot{\underline{u}}=\ddot{\underline{u}}(t^*)\ \Delta t, \qquad t^*=t_o+\Delta t/2 \tag{8a, b, c}$$

we obtain the equation

$$\Delta\underline{F}^*=\underline{K}^*\ \Delta\underline{u}+\underline{L}\ \Delta\underline{\lambda} \tag{9a}$$

with

$$\underline{K}^*=\underline{K}+\frac{4}{\Delta t^2}\ \underline{M}+\frac{2}{\Delta t}\ \underline{B}, \qquad \Delta\underline{F}^*=\Delta\underline{F}+\left\{\frac{4}{\Delta t}\dot{\underline{u}}_o+2\ \ddot{\underline{u}}_o\right\}\ \underline{M}+2\ \dot{\underline{u}}_o\ \underline{B} \tag{9b, c}$$

Thus, Eqs. (9a) and (3b) become the governing equations for the incremental dynamic elastic plastic problem. Even when $V(\Delta\underline{\lambda})$ is not convex, such equations can often be interpreted as optimality condition of a *convex, unconstrained* problem fully analogous to the problem (4), provided that $\underline{K}^*$ and $\Delta\underline{F}^*$ be used instead of K and $\Delta\underline{F}$. Indeed, in the presence of softening and, hence, of non-convex $V(\Delta\underline{\lambda})$ functions, we can consider the problem

$$\begin{aligned}\min \Big\{&\frac{1}{2\alpha^2}\ \Delta\underline{u}^T\ \underline{K}\ \Delta\underline{u}+\Delta\underline{u}^T\ \underline{L}\ \Delta\underline{\lambda}+\frac{1}{2}\ \Delta\underline{u}^T\ \underline{R}\ \Delta\underline{u}+\frac{1}{2}\ \alpha^2\ \Delta\underline{\lambda}^T\ \underline{E}\ \Delta\underline{\lambda}\\ &+\frac{(1-\alpha^2)}{2}\ \Delta\underline{\lambda}^T\ \underline{E}\ \Delta\underline{\lambda}+D(\Delta\underline{\lambda})+V(\Delta\underline{\lambda})-\{\Delta\underline{F}^*\}^T\ \Delta\underline{u}+\Delta\underline{\lambda}^T\ \underline{L}^T\ \underline{u}_o+\Delta\underline{\lambda}^T\underline{E}\ \underline{\lambda}_o\Big\}\end{aligned} \tag{10a}$$

with

$$\underline{R}=\underline{K}^*-\frac{1}{\alpha^2}\ \underline{K} \tag{10b}$$

Let us now consider the quadratic form

$$\frac{1}{2}\ \Delta\underline{y}^T\ \underline{Q}\ \Delta\underline{y}=\frac{1}{2\alpha^2}\ \Delta\underline{u}^T\ \underline{K}\ \Delta\underline{u}+\Delta\underline{u}^T\ \underline{L}\ \Delta\underline{\lambda}+\frac{1}{2}\alpha^2\ \Delta\underline{\lambda}^T\ \underline{E}\ \Delta\underline{\lambda} \tag{11a}$$

with

$$\Delta \underline{y}^T = \left[\frac{1}{\alpha} \ \Delta \underline{u}^T | \alpha \Delta \underline{\lambda}^T \right], \quad \underline{Q} = \begin{bmatrix} \underline{K} & \underline{L} \\ \underline{L}^T & \underline{E} \end{bmatrix} \tag{11b, c}$$

Note that $\underline{Q}$ is positive semidefinite, since the quadratic form on the left hand side of Eq. (11a) represents the strain energy of a discretised elastic, perfectly plastic system. Therefore, the objective function of the problem (10a) is convex if we can find a parameter α that makes the matrix

$$\left[(1-\alpha^2)\ \underline{E} + \frac{\partial^2 V}{\partial \Delta \underline{\lambda}\ \partial \Delta \underline{\lambda}^T} \right] = \text{diag} \left[(1-\alpha^2)\ \underline{E}_j + \frac{\partial^2 V}{\partial \Delta \underline{\lambda}_j\ \partial \Delta \underline{\lambda}_j^T} \right] \tag{12}$$

at least positive semidefinite. Finally, Eqs. (9b) and (10b), allow one to define an upper bound for the parameter α, beyond which the matrix $\underline{R}$ is not positive definite any more. Details on this issue are given by Rajgelj, *et al.* (1993). The same problem was originally discussed by Comi, *et al.* (1992) by considering a traditional approach centred on yield functions (rather than dissipation functions), nonlinear constrained (rather than unconstrained) optimisation problems, linear kinematic hardening and Mises' yield condition.

3. A numerical model for masonry

Here, a material model is considered that belongs to the class of models discussed in the previous Section. Hence, the same extremum properties and convergence properties are maintained. The model has been developed for masonry subjected to plane stress conditions. Thus, three stress components will be considered (say σ_{11}, σ_{22} and σ_{12}, with σ_{22} normal to the mortar beds). Tensile stresses will be assumed as positive. At first, the model will be introduced with reference to a traditional approach based upon yield functions. More specifically, a piecewise linear yield locus will be considered in the space σ_{11}-σ_{22}-σ_{12}. Fig. 4 shows a partial view of the surface. Eight yield planes are assumed in the half space $\sigma_{12} \geq 0$. One plane (shown in dark grey) takes into account possible slips along horizontal joints by assuming Coulomb friction. This plane is normal to the plane $\sigma_{11}=0$ and its equation reads

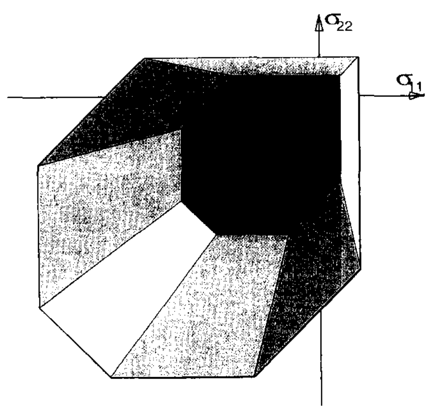

Fig. 4 Scheme of the piecewise linear yield surface.

$$\sigma_{12}=c+\phi\ \sigma_{22} \tag{13}$$

where c and ϕ represent the cohesion and the tangent of the friction angle.

Similarly, eight yield planes are assumed in the half space $\sigma_{12}\leq 0$, which are symmetrical with respect to the plane $\sigma_{12}=0$. Altogether the sixteen planes define a closed elastic domain. Convenient evolution laws can be assumed and softening effects can be included.

With reference to the formulation introduced in the previous Section, a slip device is assumed at each strain point. In addition, an associated flow rule is considered (i.e., inelastic strain increments are normal to the yield planes). Thus, the inelastic strain increment $\Delta\underline{\lambda}_j$ at the jth strain point ($j=1$, ..., m) becomes

$$\Delta\underline{\lambda}_j=\underline{N}_j\ \Delta\underline{\mu}_j \ \text{ with } \ \underline{N}_j=[\underline{n}_j^1|\underline{n}_j^2|...|\underline{n}_j^Y] \tag{14a, b}$$

where $\underline{n}_j^k$ represents the unit outward vector normal to the kth plane ($k=1$, ..., Y and $Y=16$ in this case). The vector $\Delta\underline{\mu}_j$ collects sixteen plastic multipliers $\Delta\mu_j^k$. Of course, no summation is implied in Eq. (14a). Then, the dissipation function related to each slip can be expressed in the form

$$D=\sum\nolimits_{k=1,16} r_j^k\ \Delta\mu_j^k \tag{15}$$

where r_j^k denotes the distance of the kth plane from the origin of the space σ_{11}-σ_{22}-σ_{12}.

The evolution law for the yield planes can be defined by using one function $V(\Delta\mu_j^k)$ associated to each plastic multiplier $\Delta\mu_j^k$. For instance, r_j^k-$\Delta\mu_j^k$ plots such as the ones depicted in Fig. 5 can be obtained by introducing convenient functions $V(\Delta\mu_j^k)$. If the r_j^k-$\Delta\mu_j^k$ relationship is piecewise linear, the plastic multipliers are found by solving a linear complementarity problem (Maier 1970, Maier and Nappi 1989). After determining the plastic multipliers, we can compute the inelastic strain increments $\Delta\underline{\lambda}_j$ through Eq. (14a). Such increments can be split in two parts, one non-reversible (plastic strain), one associated to damage (i.e., to a decrease of stiffness and strength). Thus, at the end of each time interval the total strain $\underline{\varepsilon}_j$ at the jth strain point reads

$$\underline{\varepsilon}_j=\underline{\varepsilon}_j^o+\underline{C}_j\ \Delta\underline{\sigma}_j+\Delta\underline{\varepsilon}_j^P+\Delta\underline{\varepsilon}_j^D \ \text{ with } \ \Delta\underline{\varepsilon}_j^D=\Delta\underline{C}_j\ \{\underline{\sigma}_j^o+\Delta\underline{\sigma}_j\} \tag{16a, b}$$

where $\underline{\varepsilon}_j^o$, $\underline{\sigma}_j^o$ and $\underline{C}_j$ denote the total strain, the stress and the compliance matrix at the beginning of the current time step. On the other hand, $\Delta\underline{\sigma}_j$, $\Delta\underline{\varepsilon}_j^P$, $\Delta\underline{\varepsilon}_j^D$ and $\Delta\underline{C}_j$ represent increments of stresses, plastic strains, additional strains associated to damage and compliance matrix. The

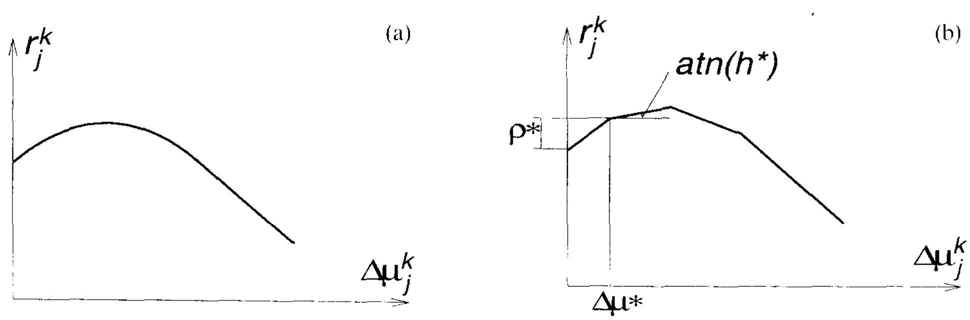

Fig. 5 Distance of a yield plane from the origin as function of the relevant. plastic multiplier (a) and piecewise linear approximation (b).

initial compliance matrix is related to the stiffness matrix in Eq. (3b): $\underline{C}_j=[\underline{E}_j]^{-1}$. In this context, $\underline{E}_j$ is to be interpreted as material stiffness matrix at the beginning of the current step (to be updated at the end of each time interval).

In order to define the matrix $\Delta\underline{C}_j$ we can proceed as follows (Papa and Nappi 1997). First, we introduce a relationship between the vectors $\Delta\underline{\varepsilon}_j^D$ and $\underline{\sigma}^*=\{\underline{\sigma}_j^o+\Delta\underline{\sigma}_j\}$, which denotes the final stress. Hence, by considering the Eucledean norms $|\Delta\underline{\varepsilon}_j^D|$ and $|\underline{\sigma}^*|$, we can set

$$\Delta\underline{\varepsilon}_j^D=|\Delta\underline{\varepsilon}_j^D|\underline{n}_\varepsilon=\rho|\underline{\sigma}^*|\underline{n}_\varepsilon=\Delta\underline{C}_j\,\underline{\sigma}^*=\Delta\underline{C}_j|\underline{\sigma}^*|\underline{n}_\sigma \tag{17}$$

where $\underline{n}_\varepsilon$ and $\underline{n}_\sigma$ are unit vectors that give the directions of $\Delta\underline{\varepsilon}_j^D$ and $\underline{\sigma}^*$, while ρ is the ratio between $|\Delta\underline{\varepsilon}_j^D|$ and $|\underline{\sigma}^*|$. Next, from Eq. (17) we immediately obtain

$$\Delta\underline{C}_j\ \underline{n}_\sigma=\rho\ \underline{n}_\varepsilon=\frac{\rho}{\underline{n}_\varepsilon^T\underline{n}_\sigma}\,[\underline{n}_\varepsilon\underline{n}_\varepsilon^T]\ \underline{n}_\sigma \rightarrow \Delta\underline{C}_j=\frac{\rho}{\underline{n}_\varepsilon^T\underline{n}_\sigma}\,[\underline{n}_\varepsilon\ \underline{n}_\varepsilon^T] \tag{18a, b}$$

In the case of dynamic structural analysis the piecewise-linear material model leads to the equations

$$\Delta\underline{F}^*=\underline{K}^*\ \Delta\underline{u}+\underline{L}\ \underline{N}\ \Delta\underline{\mu},\quad -\underline{r}=\underline{N}^T\ \underline{L}^T\ \Delta\underline{u}+\underline{S}\ \Delta\underline{\lambda}+\{\partial V/\partial\Delta\underline{\mu}\}+\underline{N}^T\ \underline{L}^T\ \underline{u}_o+\underline{N}^T\ \underline{E}\ \underline{\lambda}_o \tag{19a, b}$$

with

$$r_j^k=\partial D/\partial\Delta\mu_j^k \ \text{ if } \Delta\mu_j^k\neq 0,\ r_j^k\in\partial D(\Delta\mu_j^k) \ \text{ if } \Delta\mu_j^k=0 \tag{19c, d}$$

$$\underline{N}=\text{diag}\ [\underline{N}_j],\ \underline{S}=\underline{N}^T\ \underline{E}\ \underline{N}=\text{diag}\ [\underline{S}_j]=\text{diag}\ [\underline{N}_j^T\ \underline{E}_j\ \underline{N}_j] \tag{19e, f}$$

It should be noted that no summation is implied in Eq. (19f) and that $\underline{r}$ in Eq. (19b) collects the $m\cdot Y$ scalar quantities r_j^k. In addition, when the r_j^k-$\Delta\mu_j^k$ plots are piecewise linear, the gradient $\{\partial V/\partial\Delta\underline{\mu}\}$ is made of the m subvectors

$$\underline{\rho}_j=\underline{\rho}_j^o+\underline{H}_j\ \{\Delta\underline{\mu}_j-\Delta\underline{\mu}_j^o\} \tag{19g}$$

with $j=1, \ldots, m$. Thus, the scalar components of $\underline{\rho}_j$ give (as functions of $\Delta\underline{\mu}_j$ and for each yield plane at the jth point) the change of the distance from the origin of the stress space σ_{11}-σ_{22}-σ_{12}. The change of distance concerned with the kth plane at the jth point can be denoted as ρ_j^k. For any $\Delta\mu_j^k$, there is a characteristic slope of the r_j^k-$\Delta\mu_j^k$ plot, say h^* (cf. Fig. 5b). The branch characterised by the slope h^* starts at the point where $\Delta\mu_j^k$ and ρ_j^k attain convenient values $\Delta\mu^*$ and ρ^*. Therefore, as suggested by Fig. 5b, we can consider the equation $\rho_j^k=\rho^*+h^*$ $(\Delta\mu_j^k$-$\Delta\mu^*)$, in which the scalar quantities ρ^* and $\Delta\mu^*$ represent (for a certain value of $\Delta\mu_j^k$) the kth entries of the vectors $\underline{\rho}_j^o$ and $\Delta\underline{\mu}_j^o$ in Eq. (19g), while h^* corresponds to the kth diagonal term of the matrix H_j.

When hardening occurs, we can assume diagonal matrices H_j. Clearly, during the hardening phase all the properties pointed out in the previous Section continue to hold, since Eqs. (19a, b, c, d) represent the optimality conditions for the *convex, unconstrained problem*

$$\min\left\{\frac{1}{2}\ \Delta\underline{u}^T\ \underline{K}^*\ \Delta\underline{u}+\Delta\underline{u}^T\ \underline{L}\ \underline{N}\ \Delta\underline{\mu}+\frac{1}{2}\ \Delta\underline{\mu}^T\ \underline{S}\ \Delta\underline{\mu}\right.$$
$$\left.+D(\Delta\underline{\mu})+V(\Delta\underline{\mu})-\{\Delta\underline{F}^*\}^T\ \Delta\underline{u}+\Delta\underline{\mu}^T\ \underline{N}^T\ \underline{L}^T\ \underline{u}_o+\Delta\underline{\mu}^T\ \underline{N}^T\ \underline{E}\ \lambda_o\right\} \tag{20}$$

When softening starts to occur at a strain point (i.e., when the distance of one plane from the origin starts to decrease), we can assume the matrix

$$\underline{H}_j=\underline{H}_j^1+\underline{H}_j^2=\begin{bmatrix} h_1 & \underline{n}_1^T h_1 \underline{n}_2 & \cdots\cdots & \underline{n}_1^T h_1 \underline{n}_Y \\ \underline{n}_2^T h_1 \underline{n}_1 & h_2 & \cdots\cdots & \underline{n}_2^T h_2 \underline{n}_Y \\ \cdots & \cdots & \cdots & \cdots \\ \underline{n}_Y^T h_Y \underline{n}_1 & \underline{n}_Y^T h_Y \underline{n}_2 & \cdots\cdots & h_Y \end{bmatrix}+\text{diag}\ [\Delta h_k] \tag{21}$$

where $h_1 \leq h_2 \leq \cdots \leq h_Y$ represent, for each r_j^k-$\Delta\mu_j^k$ plot, the steepest slopes of the softening branches. On the other hand, the scalar quantities Δh_k ($k=1, ..., Y$) denote the increments to be added in order to obtain the correct slopes along the main diagonal of the matrix $\underline{H}_j$ (depending upon the particular value attained by the plastic multiplier $\Delta\mu_j^k$). Obviously, Δh_k will always be non-negative for any k.

The matrix $\underline{H}_j^1$ in Eq. (21) can be expressed in the form

$$\underline{H}_j^1=[\underline{A}_1\text{-}\underline{B}_1]+[\underline{A}_2\text{-}\underline{B}_2]+\cdots+[\underline{A}_{Y-1}\text{-}\underline{B}_{Y-1}]+\underline{A}_Y \tag{22a}$$

where

$$[\underline{A}_s\text{-}\underline{B}_s]=[\underline{M}_s]^T\ [\underline{h}_s]\ [\underline{M}_s]-[\underline{M}_{s-1}]^T\ [\underline{h}_s]\ [\underline{M}_{s+1}] \tag{22b}$$

$$\underline{M}_s=[\underline{m}_s^1|\underline{m}_s^2|\cdots|\underline{m}_s^Y],\ \underline{h}_s=\text{diag}\ [h_s] \tag{22c, d}$$

with $s=1, ..., Y$. In Eq. (22c) $\underline{m}_s^k$ coincides with $\underline{n}_j^k$ if $s \geq k$, while $\underline{m}_s^k=\underline{0}$ if $s<k$. Similarly, $\underline{m}_{s+1}^k$ coincides with $\underline{n}_j^k$ if $(s+1) \geq k$, while $\underline{m}_{s+1}^k=\underline{0}$ if $(s\text{-}1)<k$. Therefore, by noting that $\underline{M}_1=\underline{N}_j$, Eq. (22a) becomes

$$\begin{aligned}\underline{H}_j^1&=[\underline{N}_j]^T\ [\underline{h}_1]\ [\underline{N}_j]+[\underline{M}_2]^T\ [\underline{h}_2-\underline{h}_1]\ [\underline{M}_2]+\cdots+[\underline{M}_Y]^T\ [\underline{h}_Y-\underline{h}_{Y-1}]\ [\underline{M}_Y] \\ &=[\underline{N}_j]^T\ [\underline{h}_1]\ [\underline{N}_j]+\hat{\underline{H}}_j^1\end{aligned} \tag{23}$$

In the above equation, the first product on the right hand side gives a negative semidefinite matrix, while the other products lead to positive semidefinite matrices, since $h_1 \leq h_2 \leq \cdots \leq h_Y$.

At this stage we can recover the convergence property found in the previous Section. Indeed, simple manipulations (already discussed above) allow us to transform the optimisation problem (20) into the problem

$$\begin{aligned}\min \Big\{ & \frac{1}{2\alpha^2}\ \Delta\underline{u}^T\ \underline{K}\ \Delta\underline{u}+\Delta\underline{u}^T\ \underline{L}\ \underline{N}\ \Delta\underline{\mu}+\frac{1}{2}\ \Delta\underline{u}^T\ \underline{R}\ \Delta\underline{u}+\frac{1}{2}\alpha^2\ \Delta\underline{\mu}^T\ \underline{S}\ \Delta\underline{\mu}+D(\Delta\underline{\mu}) \\ & +V(\Delta\underline{\mu})+\frac{(1\text{-}\alpha^2)}{2}\ \Delta\underline{\lambda}^T\ \underline{S}\ \Delta\underline{\lambda}-\{\Delta\underline{F}^*\}^T\ \Delta\underline{u}+\Delta\underline{\mu}^T\ \underline{N}^T\ \underline{L}^T\ \underline{u}_o+\Delta\underline{\mu}^T\ \underline{N}^T\ \underline{E}\ \underline{\lambda}_o\Big\}\end{aligned} \tag{24}$$

with $\underline{R}$ defined in Eq. (10b). Further manipulations (fully analogous to those considered in the previous section) show that the objective function of the problem (24) is convex if the matrix

$$\left[(1-\alpha^2)\ \underline{S}+\frac{\partial^2 V}{\partial\Delta\underline{\mu}\ \partial\Delta\underline{\mu}^T}\right]=\text{diag}\ [(1-\alpha^2)\ \underline{S}_j+\underline{H}_j^1+\underline{H}_j^2 \tag{25a}$$

is made at least positive semidefinite. As a consequence, we simply need to make the matrix $[(1-\alpha^2)\ \underline{E}_j+\underline{h}_1]$ at least positive semidefinite, as suggested by the equation

$$(1-\alpha^2)\ \underline{S}_j+\underline{H}_j^1+\underline{H}_j^2=[\underline{N}_j]^T\ [(1-\alpha^2)\ \underline{E}_j+\underline{h}_1]\ [\underline{N}_j]+\hat{\underline{H}}_j^1+\underline{H}_j^2 \tag{25b}$$

in which $\hat{\underline{H}}_j^1$, defined in Eq. (23), and $\underline{H}_j^2$ are at least positive semidefinite.

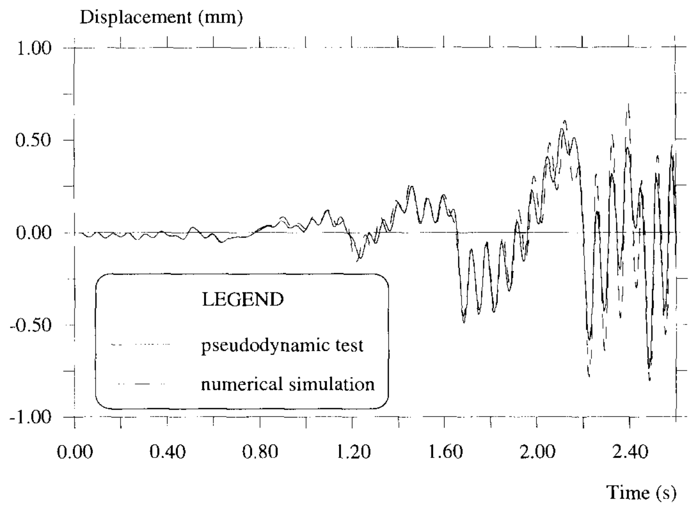

Fig. 6 Numerical response and experimental data concerned with a pseudodynamic test on a brick masonry shear wall.

4. Numerical example

A simplified version of the model was utilised for the numerical simulation of a shear brick masonry wall subjected to pseudodynamic tests at the University of Trieste in the framework of a research project originally supported by the European Commission - Environment Programme. An elastic, perfectly plastic behaviour was assumed, without taking into account hardening, softening and damage effects. The dimensions of the masonry wall were $146 \times 200 \times 39$ cm. It was constrained at the lower edge and no rotations were allowed to the upper edge. Along this edge a constant compression load was applied and horizontal displacements were imposed, as required by the computer package developed for the pseudodynamic test. The El Centro record was utilised in order to simulate a ground acceleration. The masonry panel was discretised by sixteen isoparametric eight-node elements and the constitutive law was enforced at four strain (Gauss) points in each element.

Fig. 6 compares the numerical results and the response during one pseudodynamic test. The horizontal displacement of the top edge is reported as a function of time. Reasonable matching can be noted, in spite of some discrepancy due to the crude approximation introduced by the elastic, perfectly plastic behaviour of the simplified model.

5. Closing remarks

A numerical model suitable for masonry and, in general, for rock-like materials has been presented. The model combines concepts developed in the context of Plasticity and Damage Mechanics. An internal variable approach has been applied, that gives governing equations which are centred on the use of dissipation functions, while yield functions (and consequent inequality constraints) do not explicitly appear. Thus, extremum properties are derived that involve convex unconstrained objective functions (instead of constrained optimisation problems, found with more traditional approaches based on the use of yield functions). In view of these properties, convergence can be proved of convenient prediction-correction algorithms, that use the backward difference time integration scheme. It has been shown that hardening or elastic, perfectly plastic materials are required for a straightforward proof of such properties. An extension, however, is possible in the presence of softening materials by exploiting fictitious viscous elements and (in the case of dynamic systems) inertia forces.

Next, the paper discusses the main features of the model proposed for masonry. It is characterised by piecewise linear yield surfaces and the above properties have been extended in such a way that they become applicable to the model presented here and, in general, to piecewise linear numerical models.

Finally, a simplified version of the model has been used to compute the response of a brick masonry shear wall subject to ground acceleration. The numerical results have been compared with experimental data obtained by performing a pseudodynamic test on the same shear wall.

Acknowledgements

A grant from the Italian Ministry for Universities and Scientific Research (MURST) is gratefully acknowledged.

References

Comi, C., Corigliano, A. and Maier, G. (1992), "Dynamic analysis of elastoplastic softening discretized structures", *J. Eng. Mech. ASCE*, **118**, 2352-2375.

Drucker, D.C. (1964), "On the postulate of stability of materials in mechanics of continua", *J. de mechanique*, **3**, 235-249.

Gambarotta, L. and Lagomarsino, S. (1997), "Damage models for the seismic response of brick masonry shear walls. Part II: The continuum model and its applications", *Earth. Eng. and Struct. Dyn.*, to appear.

Lourenço, P.B. (1996), *Computational Strategies for Masonry Structures*, Delft University Press, Delft, The Netherlands.

Maier, G. (1970), "A matrix structural theory of piecewise-linear plasticity with interacting yield planes", *Meccanica*, **5**, 1, 55-66.

Maier, G. and Nappi, A. (1985), "A theory of perfectly no-tension discretized structural systems", *Engineering Structures*, **12**, 227-234.

Maier, G. and Nappi, A. (1989), "Backward difference time integration, nonlinear programming and extremum theorems in elastoplastic analysis". *SM Archives*, **14**, 1, 17-36.

Maier, G., Nappi, A. and Papa, E. (1991), "Damage models for masonry as a composiste material: a numerical and experimental analysis", *Constitutive Laws for Engineering Materials* (edited by C.S. Desai, E. Krempl, G. Frantziskonis and H. Saadatmanesh), ASME Press, New York, 427-432.

Martin, J.B. (1975), *Plasticity: Fundamentals and General Results*, MIT Press, Cambridge, Mass.

Martin, J.B. (1981), "An internal variable approach to finite element problems in plasticity". *Physical Nonlinearities in Structural Analysis* (edited by J. Hutland and J. Lemaitre), Springer-Verlag, 165-176.

Martin, J.B. and Nappi, A. (1990), "An internal variable formulation for perfectly plastic and linear hardening relations in plasticity". *European J. Mech., A/Solids*, **9**, 107-131.

Martin, J.B. and Reddy, B.D. (1988), "Variational principles and solution algorithms for internal variable formulations of problems in plasticity". *Omaggio a Giulio Ceradini*, University "La Sapienza", Roma.

Nappi, A. (1991), "Application of convex analysis concepts to the numerical solution of elastic plastic

problems by using an internal variable approach". *Eng. Optimization,* **18**, 79-92.
Nappi, A. (1995), "An internal variable approach applied to boundary element elastic-plastic analysis", *Computational Mechanics '95* (edited by S.N. Atluri, G. Yagawa and T.A. Cruse), Springer-Verlag, Berlin, 2769-2774.
Page, A.W. (1978), "Finite element model for masonry", *J. Struct. Div.,* ASCE, **104**, 1267-1285.
Pande, G.N., Liang, J.X. and Middleton, J. (1989), "Equivalent elastic moduli for brick masonry", *Computer and Geotechnics,* **8**, 243-265.
Papa, E. (1996), "A unilateral damage model for masonry based on a homogenization procedure", *Mechanics of Cohesive-Frictional Materials,* **1**, 349-366.
Papa, E. and Nappi, A. (1997), "Numerical modelling of masonry: a material model accounting for damage effects and plastic strains", *Applied Mathematical Modelling,* to appear.
Rajgelj, S., Amadio, C. and Nappi, A. (1993), "An internal variable approach applied to the dynamic analysis of elastic-plastic structural systems", *Earth. Eng. and Struct. Dyn.,* **22**, 885-903.